Ecosystems (2012) 15: 213–229
DOI: 10.1007/s10021-011-9504-0

ECOSYSTEMS

The Effects of Permafrost Thaw on Soil Hydrologic, Thermal, and Carbon Dynamics in an Alaskan Peatland

Jonathan A. O'Donnell,[1]* M. Torre Jorgenson,[2] Jennifer W. Harden,[3] A. David McGuire,[4] Mikhail Z. Kanevskiy,[5] and Kimberly P. Wickland[1]

[1]*U.S. Geological Survey, 3215 Marine St., Suite E-127, Boulder, Colorado 80303, USA;* [2]*Alaska Ecoscience, Fairbanks, Alaska 99775, USA;* [3]*U.S. Geological Survey, 325 Middlefield Rd, MS 962, Menlo Park, California 94025, USA;* [4]*U.S. Geological Survey, Alaska Cooperative Fish and Wildlife Research Unit, Institute of Arctic Biology, University of Alaska Fairbanks, Fairbanks, Alaska 99775, USA;* [5]*Institute of Northern Engineering, University of Alaska Fairbanks, Fairbanks, Alaska 99775, USA*

Abstract

Recent warming at high-latitudes has accelerated permafrost thaw in northern peatlands, and thaw can have profound effects on local hydrology and ecosystem carbon balance. To assess the impact of permafrost thaw on soil organic carbon (OC) dynamics, we measured soil hydrologic and thermal dynamics and soil OC stocks across a collapse-scar bog chronosequence in interior Alaska. We observed dramatic changes in the distribution of soil water associated with thawing of ice-rich frozen peat. The impoundment of warm water in collapse-scar bogs initiated talik formation and the lateral expansion of bogs over time. On average, Permafrost Plateaus stored 137 ± 37 kg C m^{-2}, whereas OC storage in Young Bogs and Old Bogs averaged 84 ± 13 kg C m^{-2}. Based on our reconstructions, the accumulation of OC in near-surface bog peat continued for nearly 1,000 years following permafrost thaw, at which point accumulation rates slowed. Rapid decomposition of thawed forest peat reduced deep OC stocks by nearly half during the first 100 years following thaw. Using a simple mass-balance model, we show that accumulation rates at the bog surface were not sufficient to balance deep OC losses, resulting in a net loss of OC from the entire peat column. An uncertainty analysis also revealed that the magnitude and timing of soil OC loss from thawed forest peat depends substantially on variation in OC input rates to bog peat and variation in decay constants for shallow and deep OC stocks. These findings suggest that permafrost thaw and the subsequent release of OC from thawed peat will likely reduce the strength of northern permafrost-affected peatlands as a carbon dioxide sink, and consequently, will likely accelerate rates of atmospheric warming.

Key words: peatlands; soil carbon; permafrost; thermokarst; Alaska; climate change; boreal.

Received 12 July 2011; accepted 21 October 2011;
published online 17 November 2011

Author Contributions: JAO—performed research, analyzed data, wrote the paper; MTJ—designed study, performed research; JWH—conceived study, performed research; ADM—Analyzed data; MZK, KPW—performed research.

*Corresponding author; e-mail: jodonnell@usgs.gov

Introduction

Peatlands account for approximately 19% of the northern circumpolar permafrost region, and store 277 Pg of organic carbon (OC; Tarnocai and others 2009). In the subarctic, nearly 48% of soil OC is stored in frozen peat deposits (Tarnocai 2007).

Having developed over thousands of years since the last glaciation (Harden and others 1992), northern peatlands have generally functioned as long-term sinks for atmospheric carbon dioxide (CO_2) and sources of atmospheric methane (CH_4; Blodau 2002; Smith and others 2004), and have functioned to cool the atmosphere (Frolking and Roulet 2007). However, climate-driven changes in permafrost extent or wildfire frequency could reduce the sink strength of northern peatlands (McGuire and others 2010; Hayes and others 2011) through the release of OC stored in frozen or saturated peat (Turetsky and others 2002a; Dise 2009; Dorrepaal and others 2009). Permafrost degradation is of particular concern, given the recent acceleration of permafrost thaw in subarctic peatlands (Payette and others 2004; Camill 2005) and future projections of circumpolar permafrost thaw (Euskirchen and others 2006; Delisle 2007; Lawrence and others 2008).

Permafrost governs soil drainage and vegetation composition in peatlands (Camill 1999; Yoshikawa and Hinzman 2003) and, consequently, influences rates of OC storage and release from soils (Turetsky and others 2007). Permafrost thaw in peatlands typically results in the subsidence of the ground surface (that is, thermokarst) and increased saturation of surface peat. This post-thaw shift in local hydrology has been shown to drive increased rates of methane emissions (Turetsky and others 2002b; Christensen and others 2004; Wickland and others 2006) and soil OC accumulation (Robinson and Moore 1999, 2000) in thermokarst features relative to undisturbed soils. However, considerable uncertainty remains regarding the effects of permafrost thaw on soil carbon balance (Limpens and others 2008) and the magnitude of carbon cycle feedbacks to the climate system (Schuur and others 2008; McGuire and others 2009). For example, deep C stocks in peatlands may be more sensitive to warming than previously thought (Dorrepaal and others 2009), which suggests that permafrost thaw in peatlands may amplify atmospheric warming. Furthermore, the temperature sensitivity of decomposition in northern peatlands is tightly coupled to changes in peat thickness and water table (Ise and others 2008), which are also likely to change with future warming.

OC accumulation and storage is generally higher in bogs relative to other peatland types in permafrost regions (Robinson and Moore 1999; Tarnocai 2007; Hugelius and Kuhry 2009). Collapse-scar bogs are common thermokarst features in peatlands of Alaska and Canada (Thie 1974; Zoltai and Vitt 1990; Halsey and others 1995; Beilman and others 2001; Jorgenson and Osterkamp 2005), and have formed from the thawing of ice-rich, fine-grained mineral soils. These bogs are easily identifiable in peatland landscapes as circular depressions, expanding laterally over time at a rate of 0.1–0.5 m y^{-1} (Jorgenson and others 2001). Shifts in vegetation composition have been observed across collapse-scar successional ages (Camill 1999; Jorgenson and others 2001), as has the cyclic aggradation and degradation of permafrost (Zoltai 1993). OC accumulation in collapse-scar bogs is generally higher than in peat plateaus underlain by permafrost (Trumbore and Harden 1997; Robinson and Moore 2000; Myers-Smith and others 2008), due to post-thaw saturation of peat and reduced organic matter decomposition. However, uncertainty exists regarding changes in OC storage and accumulation with time since thaw, given the complex interaction of vegetation, soil thermal and carbon dynamics in northern peatlands (Robinson and Moore 2000) and given the variations in frozen substrates and their OC contents (Grosse and others 2011).

Here, we examine soil OC accumulation and loss following permafrost thaw across a collapse-scar bog chronosequence in peatlands of interior Alaska. Chronosequence studies have effectively characterized decadal to millennial scale effects of fire and deglaciation on soil OC dynamics in the boreal region (Harden and others 1992, 1997; Wang and others 2003; O'Neill and others 2003). Our primary objectives were to: (1) assess spatial and temporal variability of soil thermal regimes across a collapse-scar bog chronosequence; (2) compare soil moisture and water table across the chronosequence; and (3) evaluate the effects of permafrost thaw and collapse-scar bog evolution on soil OC accumulation and loss. To our knowledge, no studies have used thaw chronosequences in northern peatlands to assess the effects of permafrost thaw on soil thermal, hydrologic, and carbon dynamics. This approach provides a natural gradient in permafrost degradation, vegetation composition, and soil OC storage. To address the first objective, we measured soil thermal dynamics (temperature, thaw depth) and surface topography across a collapse-scar bog chronosequence and across lateral transects spanning a gradient of permafrost and soil drainage. To address the second objective, we made one-time measurements of water-surface elevations and continuously monitored soil moisture. To address the third objective, we compared OC storage among study sites, calculated rates of carbon input (I) and decomposition constants (k) using chronosequence and radiocarbon methodologies, and used a simple mass-balance model to evaluate

accumulation and loss rates associated with permafrost thaw. We discuss the implications of these findings with respect to future permafrost thaw and carbon cycle feedbacks from northern peatlands to the climate system.

Methods

Study Area

We conducted our studies in the Koyukuk National Wildlife Refuges (NWR), one of the largest lowland basins in Interior Alaska (Figure 1). Koyukuk NWR covers 14,160 km^2 of wetlands on the abandoned floodplains and drained thaw-lake basins adjacent to the Koyukuk River, and spans from the southern foothills of the Brooks Range to its confluence with the Yukon River near Galena, Alaska. Peat deposits at Koyukuk NWR are thick relative to other peatlands in Alaska, and are advantageous for studying long-term OC accumulation rates. There are abundant thermokarst features in the region, with a range of post-thaw successional stages within close proximity of each other. The Koyukuk Flats study area (N65.19°, W155.36°; datum = WGS84) is located approximately 50 km north of Galena, and was accessed via floatplane. Logistical support was provided in part from the U.S. Fish and Wildlife Service located in Galena. From 1971 through 2000, mean annual temperature in Galena averaged −3.8°C, with annual maxima occurring in July (20.4°C) and minima in January (−26.9°C; Alaska Climate Research Center, http://climate.gi.alaska.edu/). During that period, annual precipitation averaged 331 mm, with 40% of the annual precipitation falling in July through September. Snow typically covers the ground between the months of October and April, with an average maximum accumulation of 50 cm.

Permafrost at the Koyukuk Flats study area is characterized by thick deposits of syngenetically frozen peat (ranging from 1.7 to 4.1 m), which were underlain by para-syngenetic permafrost, generally consisting of ice-rich lacustrine silt (that is, limnic sediments). Syngenetic permafrost forms at the same time as sedimentation, causing the base of the active layer to aggrade upward (French and Shur 2010). While syngenetic permafrost is often considered to occur in areas of loess deposition (for example, Kanevskiy and others 2011) or alluvial sedimentation along river floodplains (for example, Shur and Jorgenson 1998), here we note the presence of syngenetic cryostructures formed in association with vertical peat accumulation (Figure 2A). Given the presence of limnic sediments, it is hypothesized that prior to peatland initiation in the early Holocene that our study area was part of a larger lake basin. Taliks, or unfrozen layers, are a common feature beneath lakes in high-latitude regions (for example, West and Plug 2008). During lake drainage and peatland initiation at Koyukuk Flats, it is likely that a lake talik froze from the side, a process referred to as para-syngenesis (French and Shur 2010). This process is reflected in our observation of inclined lenses in limnic sediments (Figure 2B). No ice wedges or other massive ice bodies were observed at this study area; however, the ice content of sediments is very high, with volumetric moisture contents varying between 50 and 90% due to segregated and pore ice. There is some evidence to suggest that collapse-scar features in the region have converted back to peat plateaus in recent millennia, as evidenced in the presence of

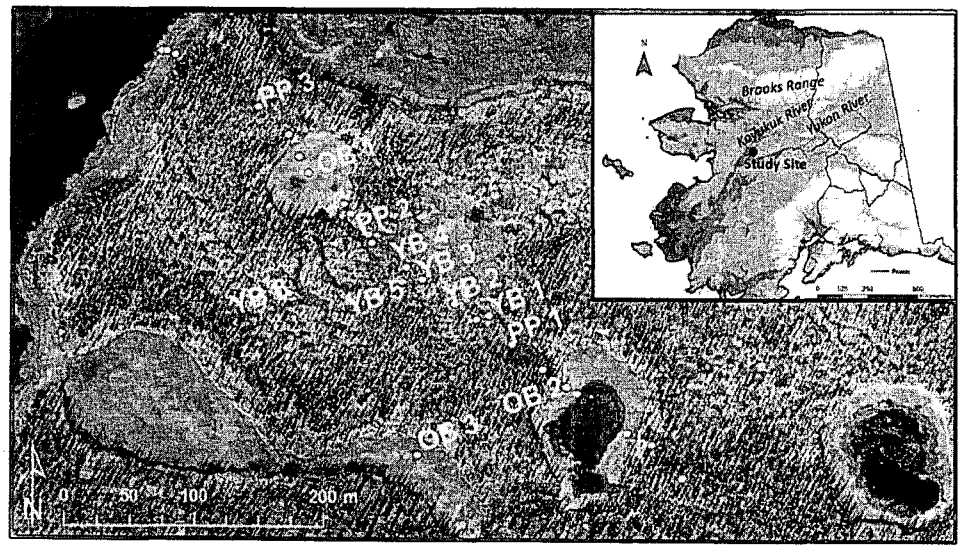

Figure 1. Map of Koyukuk Flats study region. *Open circles* represent the Permafrost Plateau (PP), Young Bog (YB), and Old Bog (OB) study sites. *Unlabeled circles* represent additional survey points along the transect where site characteristics were described but peat samples were not collected. *Inset* the location of Koyukuk Flats National Wildlife Refuge in Alaska.

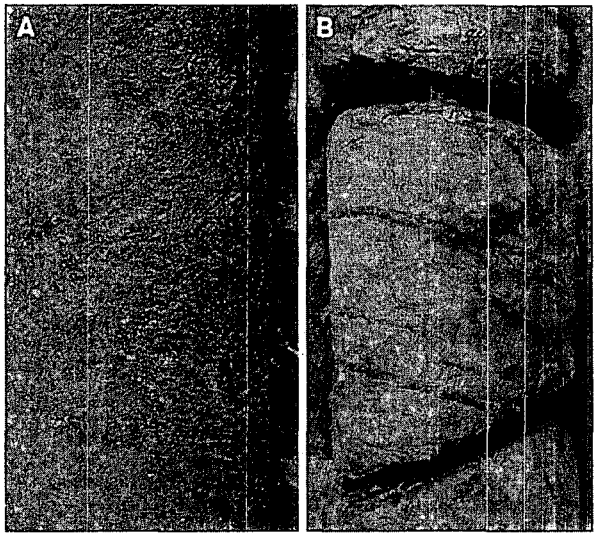

Figure 2. Permafrost cores showing typical cryostructures observed in syngenetically frozen peat (**A**) and para-syngenetically frozen lacustrine sediments (**B**).

decomposed fen peat in some Permafrost Plateau profiles.

Sampling Design

To address our study objectives, we measured soil hydrologic, thermal, and OC dynamics across a permafrost thaw chronosequence. A soil chronosequence is a series of profiles that have similar factors, such as climate, vegetation, slope, and parent material, but differ in age of the landform. Our chronosequence consisted of Permafrost Plateau sites, Drying Margin sites, and collapse-scar bogs that varied with respect to time of permafrost thaw and bog initiation (Young Bogs, Old Bogs). Bog size was used as a proxy for selected collapse-scar bogs of different ages. Although all our sites had similar climate, slope, and parent material, vegetation composition differed across landform ages, limiting our ability to isolate the effect of time from vegetation succession. The age of Young Bogs ranged from 31 to 61 years, as determined by the difference in mean age of mature black spruce trees on Permafrost Plateau sites (96 ± 13 years, $n = 9$) and the age of dead black spruce trees found in collapse-scar bog features (Table 1). Tree cores were obtained at breast-height, sanded upon returning to the laboratory, and then scanned at a resolution of 1,200 dpi. These images were then imported into CooRecorder (V.7), where the tree rings were counted manually. The age of two Old Bogs (400 and 1,215 years, respectively) was determined by radiocarbon (^{14}C) dating of organic matter at the interface of forest-derived and collapse-scar bog-derived peat (Table 2). Drying Margin sites are transitional between the Permafrost Plateau and collapse bog sites, where permafrost has begun thawing but subsidence has not yet occurred.

Vegetation composition varied with landscape position and collapse-scar bog age. Permafrost Plateaus were dominated by black spruce (*Picea mariana*) and *Sphagnum fuscum*. We commonly observed the presence of *Andromeda polifolia, Ledum decumbens,* and *Rubus chamaemorus*. Drying Margins of collapse-scar bogs were dominated by *Cladina* spp. (*C. stellaris, C. arbuscula, C. rangiferina, C. mitis*) and *L. decumbens*. Young Bogs were dominated by *Eriophorum scheuchzeri* and numerous *Sphagnum* spp., including *S. jensenii, S. riparium,* and *S. lindbergii*. In

Table 1. Summary of Collapse-Scar Bog OC Stocks and Ages

Site name	Bog C stocks (kg C m^{-2})	Forest C stocks (kg C m^{-2})	Bog or peat deposit age (years)	Age determination method
Young Bog 1	0.6	>66.5*	61	Tree ring
Young Bog 2	0.8	63.1	52	Tree ring
Young Bog 3	3.2	>8.8*	31	Tree ring
Young Bog 4	4.0	95.1	54	Tree ring
Young Bog 5	1.1	>10.0*	47	Tree ring
Young Bog 6	1.7	135.0	35	Tree ring
Old Bog 1	35.3	53.6	1,215	^{14}C
Old Bog 2	35.3	20.3	n.d.	n.a.
Old Bog 3	20.3	39.5	400	^{14}C
Permafrost Plateau 1	n.a.	77.9	7,830	^{14}C
Permafrost Plateau 2	n.a.	203.5	10,435	^{14}C
Permafrost Plateau 3	n.a.	128.1	n.d.	n.a.

**Soil profiles where we did not reach basal peat, limnic material, or silt.*
n.a. = not applicable; n.d. = not determined.

Table 2. Summary of Radiocarbon Data for Permafrost Plateau and Old Bog Sites

Depth (cm)	Horizon code	Sample description	$\delta^{13}C$ (‰)	Fraction modern	$\Delta^{14}C$ (‰)	^{14}C age (year BP)
Permafrost Plateau 1						
185	fA	Organic-rich silt with small inclusions of charred plant material	−26.1 ± 0.2	0.3773 ± 0.0007	−625.4 ± 0.7	7830 ± 20
Permafrost Plateau 2						
2	L	Live *Sphagnum fuscum*	−27.8 ± 0.2	1.0683 ± 0.0017	60.7 ± 1.7	Modern
6	D	Dead *Sphagnum* leaves and stems	−27.7 ± 0.2	1.1313 ± 0.0018	123.3 ± 1.8	Modern
10	D	Dead *Sphagnum* leaves and stems	−27.2 ± 0.2	1.2564 ± 0.0020	247.5 ± 2.0	Modern
15	D	Dead *Sphagnum* leaves and stems	−27.3 ± 0.2	1.3329 ± 0.0022	323.4 ± 2.2	Modern
25	D	Dead *Sphagnum* leaves and stems	−26.1 ± 0.2	1.2359 ± 0.0020	227.1 ± 2.0	Modern
31	F	Dead *Sphagnum* leaves and stems	−25.7 ± 0.2	0.9849 ± 0.0018	−22.1 ± 1.8	120 ± 15
50	fD	*Chamaedaphne calyculata* leaves, few Sphagnum	−27.8 ± 0.2	0.9828 ± 0.0016	−24.1 ± 1.6	140 ± 15
101	fM	Decomposed *Sphagnum* leaves and stems	−26.1 ± 0.2	0.8945 ± 0.0015	−111.9 ± 1.5	895 ± 15
210	fM	Decomposed *Sphagnum* leaves and stems	−26.9 ± 0.2	0.5906 ± 0.0010	−413.6 ± 1.0	4230 15
313	fM	Sedge roots, *Calliergon* spp. Moss	−27.5 ± 0.2	0.2972 ± 0.0007	−704.9 ± 0.7	9745 ± 20
369	fM	Detrital peat fragments	−27.2 ± 0.2	0.4132 ± 0.0008	−589.8 ± 0.8	7100 ± 15
405	fM	Fen peat, sedge leaves; *Scorpidum scorpioides* leaves and stems	−28.4 ± 0.2	0.2728 ± 0.0006	−729.2 ± 0.6	10435 ± 20
Permafrost Plateau 3						
143	fM	Dark brown frozen peat	−23.8 ± 0.2	0.4559 ± 0.0008	−547.3 ± 0.8	6310 ± 15
Old Bog 1						
2	L	Live *Sphagnum* spp.	−24.6 ± 0.2	1.0707 ± 0.0018	63.1 ± 1.8	Modern
6	L	Live *Sphagnum* spp.	−25.4 ± 0.2	1.0709 ± 0.0017	63.3 ± 1.7	Modern
10	D	Dead *Sphagnum* leaves and stems	−24.3 ± 0.2	1.0889 ± 0.0018	81.2 ± 1.8	Modern
16	D	Dead *Sphagnum* leaves and stems	−23.7 ± 0.2	1.1306 ± 0.0018	122.6 ± 1.8	Modern
20	D	Dead *Sphagnum* leaves and stems	−24.1 ± 0.2	1.1814 ± 0.0022	173.0 ± 2.2	Modern
36	D	Dead *Sphagnum* leaves and stems	−25.4 ± 0.2	0.9794 ± 0.0017	−27.6 ± 1.7	165 ± 15
52	D	Slightly decomposed *Sphagnum* stems	−25.6 ± 0.2	0.9610 ± 0.0015	−45.9 ± 1.5	320 ± 15
100	D	*Sphagnum* stems, *Chamaedaphne calyculata* leaves	−22.9 ± 0.2	0.9637 ± 0.0018	−43.2 ± 1.8	295 ± 20
147	D	*Sphagnum* stems, *Chamaedaphne calyculata* leaves	−24.9 ± 0.2	0.9637 ± 0.0015	−43.1 ± 1.5	295 ± 15
200	D	*Sphagnum* stems, *Carex limosa*	−23.2 ± 0.2	0.8925 ± 0.0016	−113.8 ± 1.6	915 ± 15
290	F	*Sphagnum* stems, *Chamaedaphne calyculata* leaves; tiny sedge or woody stems	−24.8 ± 0.2	0.8596 ± 0.0014	−146.5 ± 1.4	1215 ± 15
310	M	*Sphagnum fuscum*; *Picea mariana* wood fragment, charcoal	−25.5 ± 0.2	0.6897 ± 0.0011	−315.2 ± 1.1	2985 ± 15
Old Bog 2						
60	M	*Sphagnum* and *Carex limosa* parts	−26.1 ± 0.2	0.9843 ± 0.0016	−22.7 ± 1.6	125 ± 15
140	M	*Sphagnum* stems and leaves	−24.7 ± 0.2	0.9535 ± 0.0015	−53.3 ± 1.5	385 ± 15
292	La	Limnic sediments with sedge leaf fragments	−23.8 ± 0.2	0.6880 ± 0.0014	−316.9 ± 1.4	3005 ± 20

Table 2. Summary of Radiocarbon Data for Permafrost Plateau and Old Bog Sites

Depth (cm)	Horizon code	Sample description	$\delta^{13}C$ (‰)	Fraction modern	$\Delta^{14}C$ (‰)	^{14}C age (year BP)
Old Bog 3						
95	M	*Sphagnum* and *Caliergon* spp. and *Menyanthes trifoliata* parts	−24.9 ± 0.2	0.9517 ± 0.0018	−55.1 ± 1.8	400 ± 20
189	M	Sedge leaves, woody plant fragments	−25.7 ± 0.2	0.7101 ± 0.0014	−295.0 ± 1.4	2750 ± 20
280	M	Sedge leaves, woody plant fragments	−28.6 ± 0.2	0.3934 ± 0.0009	−609.4 ± 0.9	7495 ± 20

Note horizon codes are defined as L = live moss; D = dead moss; F = fibric organic matter; M = mesic organic matter; A = mineral soil horizon; La = limnic sediments. A lowercase f before the horizon code indicates that the soil horizon is frozen.
Note all values represent means ± one standard deviation.

the Old Bogs, we primarily observed the mosses *S. balticum* and *S. flexuosum* and shrubs *A. polifolia* and *Oxycoccus microcarpus*. Unknown moss species were sampled and sent to the Komarov Botanical Institute in St. Petersburg, Russia, for identification.

Field Sampling

To evaluate changes in local topography, permafrost and soil drainage, we established a linear transect at the Koyukuk Flats study area (522 m in length). Relative elevations of the ground and water surface were measured along the transect using an auto-level and rod in late-August 2008. At selected points along the transect (n = 210 measurements), we measured thaw depths where permafrost was present. In the absence of permafrost, we recorded the maximum observed depth of thawed soil. Along three collapse-scar bog margins, we made more intensive measurements of the permafrost table recording both probing angle and depth to demarcate talik boundaries.

We monitored soil temperature and soil moisture dynamics at the Koyukuk Flats study area to evaluate spatial variability in soil thermal conditions. From August 2008 to 2009, we monitored soil temperatures every hour using HOBO Pro V2 two-channel dataloggers (Onset Computer Corporation, Pocasset, Massachusetts, USA). Temperature was monitored at a Permafrost Plateau, Drying Margins, and Young Bog (n = 1 profile per site type). Here, we report temperature data from the ground surface (~3 cm below moss surface) and deeper in the soil profile (20–45 cm below moss surface). Volumetric water content (VWC, %) of organic soil horizons was also logged every hour at the Koyukuk Flats study area using ECH$_2$O Smart Soil Moisture probes routed to a HOBO microstation (Onset Computer Corporation, Pocasset, Massachusetts, USA). Moisture sensors were co-located with the temperature sensor profiles. At the Permafrost Plateau and Drying Margin sites, we monitored soil moisture at 5 and 25 cm below the moss surface. At the Young Bog site, we monitored soil moisture in the top 5–10 cm below the moss surface (above the water table). We also made one-time water-table depth measurements in late-August 2008 at each site across the chronosequence (n = 3 measurements per site type) to provide a snapshot of hydrologic conditions during late-summer.

Soil Carbon and Radiocarbon Inventories

We described and sampled soil horizons across collapse-scar bog chronosequences following USDA-NRCS (Soil Survey Staff 1998) and Canadian (Soil

Classification Working Group 1998) methodologies. We sampled soil from randomly selected plots at Permafrost Plateaus (n = 3), Drying Margins of Permafrost Plateaus (n = 3), Young Bogs (n = 6), and Old Bogs (n = 3). In collapse-scar bogs, we identified forest peat as organic matter derived from *S. fuscum* and *P. mariana* ecosystems commonly observed on Permafrost Plateaus, and bog peat as organic matter derived from *Sphagnum* spp. commonly observed at the surface of Young and Old Bogs (Figure 3). Fen peat horizons were typically composed of slightly decomposed moss and plant parts, such as *Drepanocladus* spp., *Calliergon* spp., *Menyanthes trifoliata*, and *Carex limosa*. Mineral soil horizons (A, B, C) were characterized for texture and the presence of buried organic material. We also described and sampled lacustrine (or limnic) sediment below peat deposits.

We used a range of tools to sample different soil horizons for chemistry, bulk density, and moisture content. At all sites, organic soil was sampled using a variety of soil knives, scissors, and corers to measure the volume of soil samples. For easily compressible, low-density samples, soil blocks were cut with scissors or serrated knives and dimensions were measured with a ruler. For less compressible shallow soils, samples were obtained with a 35-mm diameter corer rotated with a portable electric drill. For deeper unfrozen peats we used a 70-mm diameter by 130-cm long tube that was pushed and rotated into the peat by hand. A rubber cap was tightened over the corer to maintain a vacuum in the corer during extraction. At Permafrost Plateau sites, permafrost cores (up to 5 m) were obtained using a Snow, Ice, and Permafrost Research Establishment (SIPRE) corer (7.5 cm inside diameter) with a Tanaka power head. We sampled peat until either a basal mineral or limnic horizon was encountered to allow calculation of OC stocks relative to a standard basal layer across sites. We did not include organic-rich limnic soil in the OC stock calculations because we wanted to focus on OC dynamics of terrestrial ecosystems. We analyzed all soil samples for total C and nitrogen (N) using a Carlo Erba NA1500 elemental analyzer. We assumed that total carbon was equal to OC, given the low pH of soil samples (pH < 6). OC stocks were calculated by horizon type by multiplying OC concentration (% by mass), bulk density (oven-dry), and horizon thickness.

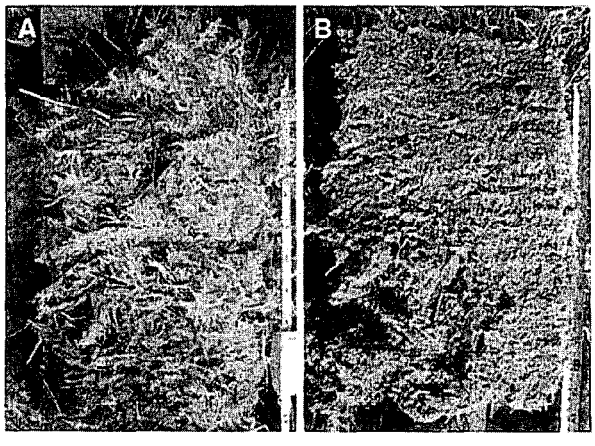

Figure 3. Comparison of bog peat (**A**) and forest peat (**B**). Bog peat colonizes collapse-scar bogs following ground subsidence and water impoundment, and is primarily composed of *Sphagnum riparium, S. balticum,* and *S. flexuosum,* with abundant live white roots of *Eriophorum scheuchzeri.* Forest peat accumulates on permafrost plateaus and then becomes submerged in collapse-scar bogs following permafrost thaw. Forest peat is composed primarily of *S. fuscum,* with abundant woody stems from *Picea mariana* and ericaceous shrubs.

We analyzed radiocarbon (^{14}C) content on a subset of soil samples to evaluate accumulation rates and turnover times of OC, to determine the age of Old Bog formation, and to determine the basal age of peat across study sites. When possible, we collected *Sphagnum* spp. moss parts for ^{14}C analysis. To determine carbon accumulation rates in Permafrost Plateaus, we analyzed the ^{14}C content of 12 organic matter samples spanning depths of 2–405 cm below the ground surface (Table 2). To age collapse-scar bogs, we analyzed ^{14}C content of organic matter at the interface of peat derived from forest and collapse-scar bog vegetation. When field sampling permitted, we also analyzed ^{14}C content of the lacustrine sediments (limnic, silt) beneath peat deposits. Samples were sent to the W.M. Keck C Cycle AMS Laboratory at the University of California Irvine for analysis as described in Southon and others (2004). Organic matter was combusted at 900°C in evacuated, sealed quartz tubes in the presence of cupric acid (CuO) and silver (Ag) wire. Following cryogenic purification, CO_2 was reduced to graphite in a reaction at 500–550°C using the sealed tube Zn reduction method (Xu and others 2007). Radiocarbon data are reported as $\Delta^{14}C$, or the per mil deviation of the $^{14}C/^{12}C$ ratio in the sample from that of an oxalic standard that has been decay corrected to 1950 (Stuiver and Polach 1977). The $\Delta^{14}C$ values we report have been corrected for mass-dependent fractionation using the in situ simultaneous AMS $\delta^{13}C$ measurement. Age interpretation of organic matter samples with modern $\Delta^{14}C$ signatures typically requires additional information, given the non-uniqueness of calculated turnover times and

ages (Trumbore 2000). We constrained our turnover time and age calculations of modern samples using literature values of soil respiration from similar ecosystems in interior Alaska (for example, mature black spruce ecosystems underlain by permafrost in Kane and others 2006).

Soil Carbon Accumulation and Loss

To quantify rates of OC accumulation at our study sites, we used both chronosequence (for example, Harden and others 1997) and radiocarbon approaches (for example, Trumbore and Harden 1997). For both methods, we assume that the net change in C storage (dC/dt) is governed by constant annual C inputs (I; kg C m^{-2} y^{-1}), the fractional first-order decomposition constant (k; y^{-1}), and OC stocks in a given year ($C(t)$). The carbon balance for any given year is reflected in the equation

$$dC/dt = I - kC(t) \quad (1)$$

Assuming that initial OC concentration is zero, solving equation (1) yields the following equation

$$C(t) = (I/k) * \left(1 - e^{-kt}\right) \quad (2)$$

For OC accumulation in shallow bog peat (which accumulates following permafrost thaw), we fit equation (2) to the relationship between bog peat across the chronosequence ($C(t)$) and bog age (t). Based on this relationship, we then determined the C input rate ($I_{shallow}$) and decomposition constant ($k_{shallow}$) for shallow bog peat. For OC accumulation at a Permafrost Plateau site prior to permafrost thaw, we fit equation (2) to the relationship between cumulative OC stocks versus radiocarbon age for the soil profile at PP2 (see Figure 1). Based on this relationship, we then determined the C input rate ($I_{permafrost}$) and decomposition constant ($k_{permafrost}$), or the C input rate and decomposition constant for the Permafrost Plateau. Change in OC stocks in forest peat following permafrost thaw is reflected by the exponential decay equation

$$C(t) = y_0 + ae^{-kt} \quad (3)$$

where y_0 is the y-intercept, a is the asymptote, k is the decomposition constant for thawed forest peat (k_{deep}), and t is time since thaw.

Mass-Balance Model of OC Accumulation and Loss

One limitation of the chronosequence approach is that the initial OC stocks in deep forest peat layers at the time of thaw are not explicitly known. Without accounting for the initial OC stocks, estimates of OC loss following permafrost thaw would likely be overestimated. To address this problem, we used a simple mass-balance model to track changes in peat OC stocks associated with permafrost aggradation and degradation. We used a "forward"-modeling approach (for example, Zhuang and others 2002), with thermokarst events scheduled at specific times during the model run to reflect collapse-scar bog formation dates observed across the chronosequence. The model operates on annual time-steps, with changes in OC stocks calculated by equation (1), and functions similarly to other mass-balance models developed for boreal study sites (for example, Harden and others 2000; O'Donnell and others 2011). Before introducing the impacts of thermokarst on soil OC stocks, we ran the model starting at 7,000 y BP, reflecting the approximate age of peatland initiation. Pre-thaw OC accumulation rates were modeled using $I_{permafrost}$ and $k_{permafrost}$ determined from the Permafrost Plateau (see above). To introduce the effects of permafrost thaw on peat carbon dynamics, we scheduled thermokarst events at 1,200, 400, and 60 y BP to reflect to the formation of Old, Intermediate, and Young collapse-scar bogs, respectively. Following a thermokarst event, the model separately tracked the accumulation of new OC in surface bog peat and loss of thawed OC from inundated forest peat. Post-thaw OC accumulation rates in shallow bog peat were modeled using $I_{shallow}$ and $k_{shallow}$ as determined from OC stocks in bog peat across the collapse-scar bog chronosequence (see above). Post-thaw OC loss rates from forest peat were modeled using k_{deep} as determined from OC stocks in forest peat across the chronosequence.

We conducted a Monte Carlo uncertainty analysis to evaluate uncertainty associated with post-thaw OC accumulation and loss. Using the mass-balance model described, a separate uncertainty analysis was conducted for an Old Bog, Intermediate Bog, and Young Bog scenario. We generated a probability distribution of each parameter ($I_{shallow}$, $k_{shallow}$, and k_{deep}) based on the observed distributions from the present study. We then ran the model 2,000 times by randomly selecting parameter values from these distributions, and evaluated the distribution of model output by reporting the range of estimates between the 5th and the 95th percentiles.

Statistical Analysis

Water-table depth was analyzed using a one-way analysis of variance (ANOVA) fixed effects model with site as the main effect. Soil OC stocks

(kg C m^{-2}) were analyzed using a two-way ANOVA fixed effects model with site (Permafrost Plateau, Young Bog, Old Bog) and peat type (bog peat, forest peat) as main effects. OC density (g C cm^{-3}), total nitrogen (TN) density (g N cm^{-3}), and C:N ratio were analyzed using a one-way ANOVA fixed effects model with soil type (Permafrost Plateau forest peat, Drying Margin forest peat, collapse-scar bog peat, collapse-scar fen peat, collapse-scar forest peat, limnic sediments, and silt) as the main effect. The two-way ANOVA models also included interactions between main effects. We used Tukey's honestly significant difference (HSD) test for post hoc comparisons of means. All statistical analyses were conducted using Statistica software (Statsoft, Inc., Tulsa, Oklahoma, USA).

Results

Soil Temperature Patterns

Thaw depth varied spatially across the study area with respect to local variability in relief and permafrost degradation (Figure 4). On Permafrost Plateaus, thaw depth was generally shallow, ranging from 30 to 70 cm. In collapse-scar bog sites (Young and Old Bogs), we generally did not observe the presence of permafrost in the top 3–4 m. However, we did contact permafrost at 251 cm in one Young Bog (YB 6 in Figure 1). We observed abrupt boundaries between the presence of permafrost on the Drying Margins of Permafrost Plateaus and the absence of permafrost in bogs (Figures 4, 5). By probing for permafrost at varying angles along collapse-scar margins, we were able to demarcate talik boundaries. We detected lateral thawing of permafrost at depths of 3–4 m below the ground surface (Figure 5).

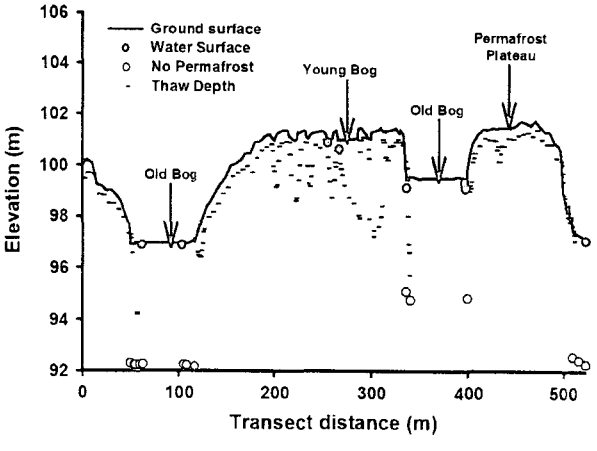

Figure 4. Variation in ground surface relief, thaw depth, and water table depth across a linear transect at the Koyukuk Flats study region.

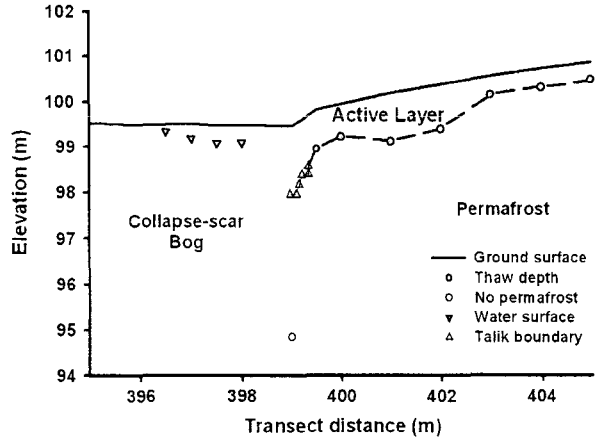

Figure 5. Talik development along collapse-scar bog margin at Koyukuk Flats study region. The talik boundary demarcates the lateral interface between thawed and frozen soil.

Mean annual temperature (MAT) at the ground surface was higher at a Young Bog feature (4.6°C) than at the Drying Margin (2.3°C) or the Permafrost Plateau (2.5°C; Figure 6A). MAT at the base of the active layer (45 cm) of the Permafrost Plateau was 0.1°C (Figure 6B), resulting in a thermal offset of −2.4°C between ground surface and permafrost table. MAT at the base of the active layer of the Drying Margin (active layer depth = 44 cm) was −0.7°C, resulting in a thermal offset of −3.0°C. MAT at 20 cm in the Young Bog was 2.7°C, with winter temperatures not dropping below 0°C.

Soil Water Dynamics

Water-table depth varied significantly (ANOVA, df = 3, $F = 21.54$, $P < 0.0001$) across the chronosequence study sites. Based on one-time measurements at replicate chronosequence sites, water-table depth averaged 35 ± 8 and 51 ± 8 cm below the ground surface at Drying Margins and Permafrost Plateaus, respectively. Water-table depth was significantly higher at Young and Old Bogs than at Permafrost Plateaus and Drying Margins (Tukey HSD test, $P < 0.05$), collectively averaging 7 ± 1 cm below the ground surface.

On average, VWC % (at 5 cm below the moss surface) was lower at the Permafrost Plateau (summer mean = 7.8 ± 0.0%, where summer is June, July, and August) than the Drying Margin (summer mean = 22.5 ± 0.1%) or the Young Bog (summer mean = 44.4 ± 0.2%; Figure 6C). On average, deep VWC (25 cm below the moss surface) was lower at the Drying Margin (summer

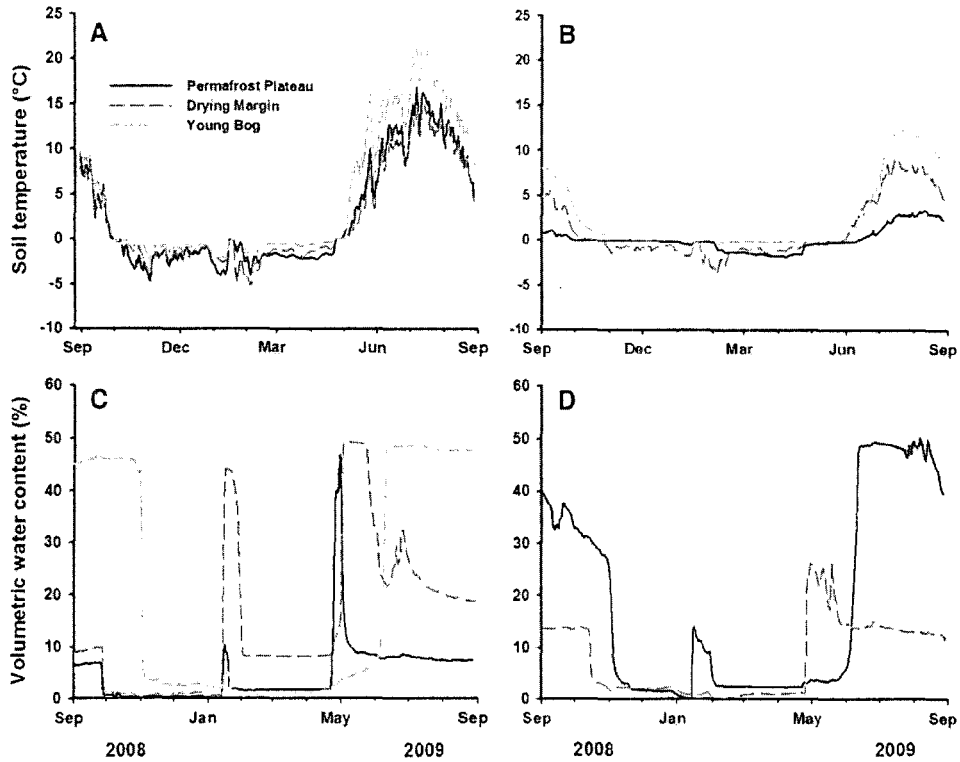

Figure 6. Seasonal variation in soil temperature at the ground surface (**A**) and deeper in the soil profile (**B**) in VWC of shallow organic horizons (**C**) and deep organic soil horizons (**D**) at a Permafrost Plateau, Drying Margin, and Young Bog site at the Koyukuk Flats study region. Deep soil temperatures were measured at 45 cm for the permafrost plateau, 45 cm for the drying margin, and 20 cm for the collapse-scar bog.

mean = 13.4 ± 0.0%) than at the Permafrost Plateau (summer mean = 44.2 ± 0.2%; Figure 6D). Since the water table was typically about 10 cm below the moss surface, we did not monitor deep VWC at the Young Bog.

Soil Carbon and Radiocarbon Inventories

Soil OC stocks varied by a significant interaction (ANOVA; df = 1, $F = 7.71$, $P = 0.016$) between site (Permafrost Plateau, Young Bog, Old Bog) and soil type (bog peat vs. forest peat; Table 1). Soil OC in the forest peat layer of the Permafrost Plateau sites averaged 137 ± 37 kg C m^{-2}, which was significantly greater than forest peat stocks at the Old Bog sites (38 ± 10 kg C m^{-2}; Tukey's HSD test, $P = 0.01$), but not significantly different than the Young Bog sites (98 ± 21 kg C m^{-2}; $P = 0.52$). At the Young Bogs, soil OC stocks were significantly higher in the forest peat layer than in the bog peat layer ($P = 0.003$), whereas in the Old Bogs, we observed no significant difference between OC stocks in bog and forest peat layers ($P = 0.99$).

OC density varied significantly (ANOVA, df = 6, $F = 11.563$, $P < 0.0001$) with soil type across the collapse-scar bog chronosequence. OC density of collapse-scar bog peat was significantly lower than forest peat from Permafrost Plateau sites (Tukey's HSD test; $P = 0.003$) and submerged forest peat ($P < 0.001$; Table 3). Silt and collapse-scar bog peat had the lowest OC density across soil types, averaging 0.02 ± 0.00 and 0.01 ± 0.00 g cm^{-3}, respectively. Total nitrogen (TN)

Table 3. Summary of Organic Matter Chemistry Across Different Soil Types

Site and soil type	*n*	OC density (g C cm^{-3})	TN density (g N cm^{-3})	C:N
Permafrost Plateau forest peat	89	0.0381 ± 0.0026^{a}	0.0011 ± 0.0001^{ab}	61 ± 4^{a}
Drying Margin forest peat	30	0.0700 ± 0.0272^{b}	0.0010 ± 0.0002^{ab}	69 ± 6^{a}
Collapse-scar bog peat	113	0.0131 ± 0.0009^{c}	0.0003 ± 0.0000^{c}	59 ± 2^{a}
Collapse-scar fen peat	7	0.0724 ± 0.0038^{ab}	0.0038 ± 0.0001^{d}	21 ± 3^{b}
Collapse-scar forest peat	115	0.0351 ± 0.0020^{a}	0.0008 ± 0.0001^{b}	58 ± 2^{ab}
Limnic sediments	12	0.0954 ± 0.0192^{b}	0.0036 ± 0.0009^{d}	37 ± 7^{b}
Silt	19	0.0218 ± 0.0026^{ac}	0.0017 ± 0.0002^{a}	12 ± 0^{b}

Note different letters denote statistically significant differences between means, as determined by Tukey's HSD test.

density also varied significantly (df = 6, $F = 36.605$, $P < 0.0001$) with respect to soil type. Across all soil types, TN density of collapse-scar bog peat was the lowest, averaging 0.0003 ± 0.0000 g cm^{-3}, whereas collapse-scar fen peat and limnic sediments had the highest TN density (Table 3).

We observed positive $\Delta^{14}C$ values in surface peat at both a Permafrost Plateau site (PP2 in Figure 1) and an Old Bog site (OB1 in Figure 1), reflecting the fixation of bomb-spike ^{14}C–CO_2 via moss production (Table 2). At both sites, $\Delta^{14}C$ peaked between 15 and 20 cm below the moss surface. $\Delta^{14}C$ generally declined with depth at the Permafrost Plateau and at the Old Bog, reflecting an increase in the age of organic matter with depth. Peatland formation was likely initiated in the early Holocene, with basal ^{14}C ages generally ranging between 7 and 10 ky BP. Based on our limited measurements, it appears that collapse-scar bogs began forming at least 1,200 y BP.

Soil Carbon Accumulation and Loss

OC inputs (I) and decomposition constants (k) varied considerably between frozen peat of the Permafrost Plateau and unfrozen peat across the collapse-scar bog chronosequence (Figure 7; Table 4). Using equation (2), we calculated that $I_{shallow}$ was greater than $I_{permafrost}$, averaging 61 ± 2 and 23 ± 8 g C m^{-2} y^{-1}, respectively. For decomposition constants, we calculated that $k_{shallow}$ was greater the $k_{permafrost}$, averaging 0.0014 ± 0.0004 and 0.0001 ± 0.0001 y^{-1}, respectively. Using equation (3), we estimate an average of 0.0140 ± 0.0093 y^{-1} for k_{deep}.

I and k parameters for different soil types were incorporated into a simple mass-balance model to simulate OC accumulation and loss associated with permafrost thaw (Figure 8A). At the Permafrost Plateau, our simulation showed that 117 kg C m^{-2} accumulated in frozen peat and unfrozen active layer soils between the time of peatland initiation (7,000 y BP) until the first development of a collapse-scar bog (1,200 y BP). Following permafrost thaw and Old Bog formation, total OC stocks declined by 48% over the next 300 years, after which OC losses slowed. Between 1,200 and 400 y BP, an additional 23 kg C m^{-2} accumulated at the Permafrost Plateau, resulting in a total of 140 kg C m^{-2} at the time of permafrost thaw and Intermediate Bog formation. Following permafrost thaw and Intermediate Bog formation, total OC stocks declined by 57% over the next 300 years. For the Young Bog, total OC stocks also declined rapidly following permafrost thaw. For each scenario, large OC losses from thawed forest peat offset the net accumulation of OC in shallow bog peat, as implied by the observations in Figure 7B.

In our Monte Carlo analysis, uncertainties associated with post-thaw OC dynamics were due to variations in $I_{shallow}$, $k_{shallow}$, and k_{deep}. The range of uncertainty associated with modeled OC stocks varied with respect to bog age (Figure 8B–D). Using the difference between OC stocks at the time of

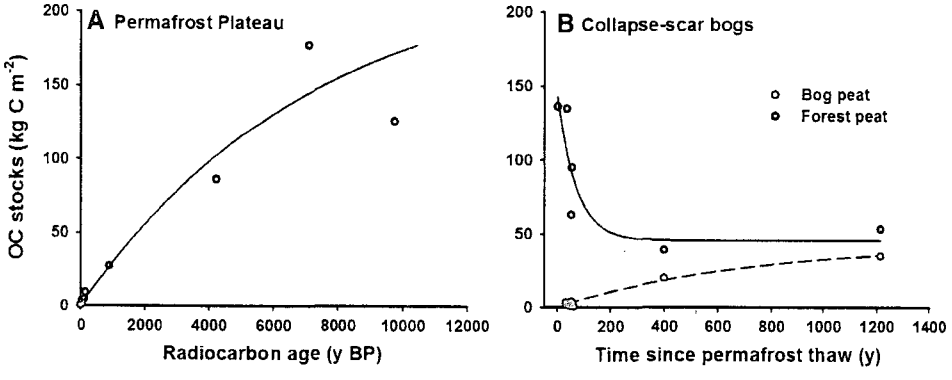

Figure 7. **A** Accumulation of OC at a Permafrost Plateau site as determined by fitting equation (2) to the relationship between cumulative OC stocks and radiocarbon age. **B** Comparison of forest and bog peat stocks over time since permafrost thaw at Koyukuk Flats study region. Bog peat, which accumulates following thaw in collapse-scar bog features, is composed primarily of *Sphagnum riparium* and *S. balticum*. The inundated forest peat layer refers to the organic matter originally accumulated and stored in soils of permafrost plateaus, which ultimately becomes saturated and buried following permafrost thaw. Forest peat is derived primarily from *S. fuscum* and ericaceous shrubs. Points at $t = 0$ reflect OC stocks from permafrost plateau profiles ($n = 3$). Where $t > 0$ points reflect collapse-scar bog age as determined via tree-ring or radiocarbon methodologies. Accumulation of OC in bog peat was determined using equation (2), whereas loss of OC from forest peat is reflected by equation (3).

Table 4. Summary of Peat Carbon Accumulation Parameters and Statistics for Koyukuk Flats Study Region

	I (g C m^{-2} y^{-1})	k (y^{-1})	R^2	P
Permafrost Plateau[a]				
Observed data	23 ± 8	0.0001 ± 0.0001	0.93	<0.0001
Model input	15	0.0001		
Shallow bog peat[b]				
Observed data	61 ± 2	0.0014 ± 0.0004	0.98	<0.0001
Model input	61	0.0018		
Thawed forest peat[c]				
Observed data	–	0.0140 ± 0.0093	0.78	0.10
Model input	–	0.0047		

Note values represent mean ± one standard deviation.
[a] $I_{permafrost}$ *and* $k_{permafrost}$ *parameters calculated by fitting equation (2) to the relationship between soil OC and* ^{14}C *age at Permafrost Plateau 2 (see Figure 7A; Table 2).*
[b] $I_{shallow}$ *and* $k_{shallow}$ *parameters calculated by fitting equation (2) to the relationship between soil OC and collapse-scar bog age across the chronosequence in Figure 7B.*
[c] k_{deep} *calculated by fitting equation (3) to the relationship between inundated forest peat and collapse-scar bog age across the chronosequence in Figure 7B.*

thaw and OC stocks at either the 95th or the 5th percentile, we calculated a range of possible loss rates. For the Young Bog, OC loss rates ranged between 178 and 1,389 g C m^{-2} y^{-1} over the 60 years following thaw (Figure 8B). For the Intermediate Bog, OC loss rates ranged between 99 and 205 g C m^{-2} y^{-1} over the 400 years following thaw (Figure 8C). For the Old Bog, OC loss rates ranged between 1 and 40 g C m^{-2} y^{-1} over the 1,200 years following thaw (Figure 8D).

Discussion

Effects of Permafrost Thaw on Hydrologic and Soil Thermal Dynamics

Collapse-scar bogs at Koyukuk Flats NWR form in response to thawing of ice-rich peat deposits and subsequent subsidence of the ground surface. The formation of these collapse-scar bogs appears to initiate a series of positive feedbacks that accelerate rates of permafrost thaw (Jorgenson and others 2010). Following ground subsidence, soil water drains laterally from the margins of Permafrost Plateaus into collapse-scar bogs, where it is impounded. We observed lateral differences in soil temperature between collapse-scar bogs and adjacent Permafrost Plateaus, which we interpret as a contributing effect of water redistribution. Spatial differences in soil temperature are related in part to the formation of taliks, which develop vertically and laterally beneath collapse-scar bog features. Talik development at depth results in further collapse and ground subsidence, and thus lateral expansion of the collapse-scar bog. Meanwhile, the spatial variability of near-surface ground temperatures reflects depths and distributions of subsurface permafrost and water tables. For example, temperature variations in this study are consistent with the findings of Jorgenson and others (2001), who observed warmer ground temperatures (at 3 m) in collapse-scar bogs and fens than in adjacent lowland black spruce stands. The presence of shallow water bodies (lakes) have been shown to have a profound influence on the ground thermal regime and permafrost in arctic tundra (Lachenbruch and others 1962; Burn 2005; West and Plug 2008; Jorgenson and others 2010). However, few studies have characterized the effect of soil water on the ground thermal conditions in subarctic peatlands, where permafrost is actively degrading (Jorgenson and others 2001).

Permafrost thaw and lateral redistribution of soil water created a drying zone along the margins of Permafrost Plateaus, evident in the reduced soil moisture content at depth relative to the wet central portions of the Permafrost Plateaus (Figure 6D) and in the colonization of lichens (*Cladina* spp.) on top of *Sphagnum fuscum* along Drying Margins. Viewed from a vertical or one-dimensional perspective, it would appear that the permafrost beneath Drying Margins is relatively stable, given the large thermal offset between the permafrost table and the ground surface (Figure 6A, B) and the shallow thaw depths. However, from a two-dimensional perspective, it becomes clear that permafrost along the Drying Margins of Permafrost Plateaus is vulnerable to thaw from lateral degradation, as discussed above. Thermal models have begun to address issues of talik development and freeze-up in association with thaw-lake cycles in Arctic regions (Ling and Zhang 2003, 2004; West and Plug 2008). Findings from this study highlight the need for thermal models that address this two- and three-dimensional complexity of permafrost degradation in northern peatlands as well.

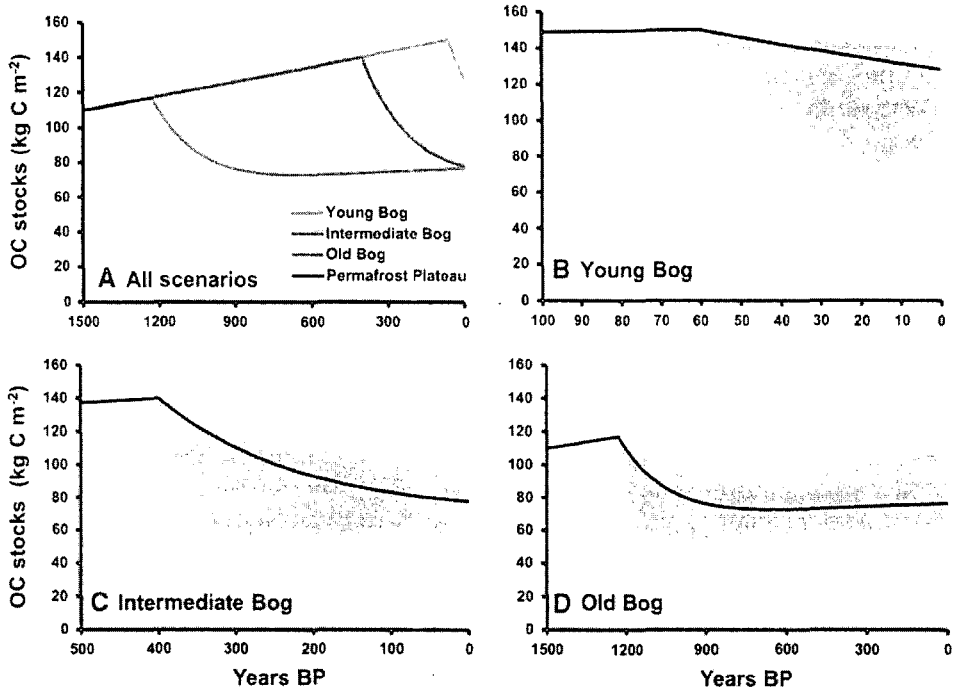

Figure 8. **A** Results from mass-balance model simulation tracking the fate of soil OC stocks following permafrost thaw and collapse-scar bog formation. Thermokarst events were scheduled at 1,200, 400, and 60 y BP to simulate the response of Old, Intermediate, and Young Bogs, respectively. **B–D** Results from Monte Carlo uncertainty analysis to evaluate post-thaw soil OC dynamics in the entire peat column for different collapse-scar bog ages. The *solid black lines* represent results from model simulation as reported in panel (**A**). The *gray shaded* areas represent the range of estimates between the 5th and the 95th percentiles. Parameters contributing to this uncertainty analysis include $l_{shallow}$, $k_{shallow}$, and k_{deep}.

Effects of Permafrost Thaw on Peatland C Dynamics

Permafrost Plateaus at the Koyukuk Flats have accumulated large amounts of OC in thick peat deposits over the past 10,000 years, with OC stocks averaging 137 ± 37 kg C m^{-2}. These measurements are consistent with other reports of OC storage in frozen peat deposits of the subarctic (Tarnocai 2007), suggesting that Permafrost Plateaus are important sinks for atmospheric CO_2 across the North American boreal region. OC stabilization in soils of Permafrost Plateaus was likely facilitated by the upward aggradation of permafrost that coincided with the accumulation of peat deposits. This process, referred to as syngenetic permafrost aggradation, was reflected in the microlenticular cryostructures that we observed in frozen peat deposits (Figure 2A). As a result, soil OC at the base of the active layer was continually incorporated into the permafrost pool, where organic matter decomposition likely ceased due to sub-zero temperatures and minimal unfrozen water content (Rivkina and others 2000; Romanovsky and Osterkamp 2000). Using equation (2), we calculate a net accumulation rate of 23 g C m^{-2} y^{-1} over the last 100 years, which is consistent with prior studies of permafrost landforms in boreal peatlands (Robinson and Moore 1999, 2000; Turetsky and others 2007; Myers-Smith and others 2008).

Following permafrost thaw and collapse-scar bog formation, shallow and deep peat horizons follow distinct trajectories, with the accumulation of OC occurring in near-surface bog peat layers and loss of OC from deep forest peat layers. Using equation (2), we calculate a net accumulation rate of 57 g C m^{-2} y^{-1} over the last 100 years, which is more than double the recent rate of accumulation at the Permafrost Plateau. This pattern of increasing OC accumulation with permafrost thaw has been observed in prior studies of sub-arctic peatlands (Robinson and Moore 1999; Turetsky and others 2007; Myers-Smith and others 2008), and reflects post-thaw changes in local hydrology.

We also observed a rapid decline of OC stocks in deep peat layers following permafrost thaw that was presumably related to increased decomposition driven by recent thawing of the forest peat. It is likely that warmer temperatures and phase change following permafrost thaw drive the rapid decom-

position of relatively labile OC in the decades and centuries following thaw. Over time, however, decomposition of the remaining substrate slows, with nearly one-half of the total forest-derived OC persisting over long periods. This observation is consistent with modeling studies (Clymo and others 1998; Frolking and others (2001, 2010), in which peat decomposition rates vary with organic matter age and depth. However, the deep peat in these collapse-scar bogs originated as "forest peat" (*S. fuscum*), which had likely undergone minimal decay following incorporation into the permafrost pool. As forest peat stocks thawed and became saturated in collapse-scar bogs, decomposition of this old, yet unprocessed organic matter was able to proceed, driving OC loss from deep peat. In addition to the effects of temperature and organic matter chemical composition, microbial abundance and activity may limit rates of organic matter decomposition in permafrost soils (Waldrop and others 2010). Post-thaw colonization of microbes from the active layer may therefore promote rapid decomposition of recently thawed OC.

Sources of Uncertainty for Peatland C Balance

The effects of permafrost thaw on the OC balance of boreal peatlands remain a key uncertainty in our ability to assess the magnitude and timing of carbon-cycle feedbacks from high-latitude regions to the climate system. In collapse-scar bog ecosystems, the net effect of permafrost thaw on the soil OC balance is governed by both OC accumulation rates in shallow bog peat and OC loss rates from thawed forest peat. We conducted a Monte Carlo uncertainty analysis to evaluate the effects of parameter uncertainty on OC stocks following permafrost thaw, as determined by processes in shallow bog peat ($I_{shallow}$, $k_{shallow}$) and thawed forest peat (k_{deep}). Findings from the Monte Carlo analysis indicate that permafrost thaw results in a net loss of OC from the entire peat column across all collapse-scar bog ages (Figure 8). However, we observed a wide range of possible outcomes, with considerable uncertainty associated with the magnitude of OC loss following thaw. Much of this uncertainty is likely driven by decomposition rates of OC in thawed forest peat, given the large error values associated with the observed k_{deep} (Table 4). Although several recent studies have improved our understanding of processes governing OC dynamics in deep peat horizons (Ise and others 2008; Dorrepaal and others 2009), more research is needed to better constrain the magnitude and timing of OC loss rates from deep peat following permafrost thaw and projected warming.

Our estimates of soil C accumulation and loss depend substantially on accurate age estimations of peat within soil profiles. In this study, we used a combination of ^{14}C and tree-ring methodology to estimate collapse-scar bog age and to calculate soil C accumulation and loss across the chronosequence. Prior studies have documented the challenge of accurately estimating peat age using ^{14}C dating (for example, Nilsson and others 2001), citing several processes that may obscure the "true" age of peat formation. For instance, deep penetrating roots can transfer comparatively young C (^{14}C age of 3–18 years, as reported by Gaudinski and others 2000) to older peat horizons. Similarly, vertical mixing of peatland porewater can introduce young dissolved organic matter into old peat horizons (Waddington and Roulet 1997), reducing the ^{14}C age of bulk peat. In permafrost settings, cryoturbation and frost cracking can also drive the redistribution of young organic matter from surficial to deeper soil horizons. At Koyukuk Flats, we also observed the downward mixing of terrestrial detritus into limnic sediments, which can complicate interpretation of peatland initiation dates. Given these complexities, there is some degree of uncertainty in our estimates of collapse-scar bog age across the chronosequence. To minimize this uncertainty, we typically sampled *Sphagnum* spp. moss parts (Table 2), which most closely approximate the true age of peat deposits (Nilsson and others 2001). Further laboratory procedures to minimize contamination by modern C, such as through acid–base–acid pre-treatment (Olsson 1986), are recommend to ensure accuracy of peat dating.

Scaling Issues and Collapse-Scar Bog Ecosystems

Collapse-scar bog formation following permafrost thaw has the capacity to fundamentally alter soil thermal, hydrologic, and carbon dynamics in lowland basins of the boreal region, as documented in this study. However, there are inherent challenges in extrapolating our observations to the regional or circumboreal scale, particularly given the spatial heterogeneity of collapse-scar features and complexity of post-thaw successional processes. Jorgenson and others (2007) report that lowlands account for approximately 42% of Alaska's boreal region, or 574,000 km^2 (Van Cleve and others 1983). Within the lowland areas, thermokarst features comprise 6% of the landscape, with collapse-scar bogs only accounting for 0.8% of the area. However, Jorgenson

and others (2007) also suggest that nearly 13% of the landscape may be susceptible to collapse-scar bog formation. For Canadian peatlands, Tarnocai (2006) predicts that up to 87% of perennially frozen peatlands (365,000 km^2) will undergo thaw by 2100, likely resulting in abundant collapse-scar bog formation. Together with these studies, our observations suggest that with continued warming collapse-scar bog development may be responsible for substantial loss of deep OC stocks from boreal peatlands.

Conclusions

Our findings document changes in soil thermal, hydrologic, and carbon dynamics following permafrost thaw in an Alaskan peatland ecosystem. The formation of collapse-scar bogs following degradation of ice-rich peat initiated substantial changes in soil OC dynamics. Accumulation of OC in shallow bog peat layers coincided with substantial loss of OC from deep forest peat layers, resulting in a net reduction in OC stocks from the entire peat column. Using a mass-balance model and uncertainty analysis, we showed that the magnitude and timing of OC loss following thaw was highly sensitive to OC input rates, decomposition constants, and collapse-scar bog age. Although our results suggest that post-thaw OC loss from these ecosystems may function as a positive feedback to atmospheric warming, future research should aim to provide regional-scale estimates of OC loss from thawed peatlands of the northern circumpolar permafrost region.

ACKNOWLEDGMENTS

Many thanks to Pedro Rodriguez for laboratory assistance, Kristen Manies for help with data processing, Trish Miller for help in the field, and Tom Douglas for sharing laboratory space. We would like to thank Stephanie Ewing, Kris Johnson, Vladimir Romanovsky, Eran Hood, and two anonymous reviewers for their valuable comments on earlier versions of this manuscript. Koyukuk NWR helped with logistical support. Funding and support for J. O'Donnell was provided by the National Science Foundation collaborative Grant EAR-0630249, the Institute of Northern Engineering at the University of Alaska Fairbanks, and the U.S. Geological Survey Global Change program.

REFERENCES

Beilman DW, Vitt DH, Halsey LA. 2001. Localized permafrost peatlands in western Canada: definitions, distribution, and degradation. Arct Antarct Alp Res 33:70–7.

Blodau C. 2002. Carbon cycling in peatlands—a review of processes and controls. Environ Rev 10:111–34.

Burn CR. 2005. Lake-bottom thermal regimes, western Arctic coast, Canada. Permafrost Periglac Process 16:355–67.

Camill P. 1999. Patterns of boreal permafrost peatland vegetation across environmental gradients sensitive to climate warming. Can J Bot 77:721–33.

Camill P. 2005. Permafrost thaw accelerates in boreal peatlands during late-20th century climate warming. Clim Change 68:135–52.

Christensen TR, Johansson T, Akerman HJ, Mastepanov M, Malmer N, Friborg T, Crill P, Svensson BH. 2004. Thawing of sub-arctic permafrost: effects on vegetation and methane emissions. Geophys Res Lett 31. doi:10.1029/2003GL018680.

Clymo RS. 1984. The limits to peat bog growth. Philos Trans Roy Soc Lond B 303:605–54.

Clymo RS, Turunen J, Tolonen K. 1998. Carbon accumulation in peatlands. Oikos 81:368–88.

Delisle G. 2007. Near-surface permafrost degradation: how severe during the 21st century? Geophys Res Lett 34. doi:10.1029/2007GL029323.

Dise NB. 2009. Peatland response to global change. Science 326:810–11.

Dorrepaal E, Toet S, van Logtestijn RSP, Swart E, van de Weg MJ, Callahan TV, Aerts R. 2009. Carbon respiration from subsurface peat accelerated by climate warming in the subarctic. Nature 460. doi:10.1038/nature08216.

Euskirchen ES, McGuire AD, Kicklighter DW, Zhuang Q, Clein JS, Dargaville RJ, Dye DG, Kimball JS, McDonald KC, Melillo JM, Romanovsky VE, Smith NV. 2006. Importance of recent shifts in soil thermal dynamics on growing season length, productivity and carbon sequestration in terrestrial high-latitude ecosystems. Glob Change Biol 12:731–50.

French H, Shur Y. 2010. The principles of cryostratigraphy. Earth Sci Rev 101:190–206.

Frolking S, Roulet NT. 2007. Holocene radiative forcing impact of northern peatland carbon accumulation and methane emissions. Glob Change Biol 13:1079–88.

Frolking S, Roulet NT, Moore TR, Richard PJH, Lavoie M, Muller SD. 2001. Modeling northern peatland decomposition and peat accumulation. Ecosystems 4:479–98.

Frolking S, Roulet NT, Tuittila E, Bubier JL, Quillet A, Talbot J, Richard PJH. 2010. A new model of Holocene peatland primary production, decomposition, water balance, and peat accumulation. Earth Syst Dyn 1:1–21.

Gaudinski JB, Trumbore SE, Davidson EA, Zheng S. 2000. Soil carbon cycling in a temperate forest: radiocarbon-based estimates of residence times, sequestration rates and partitioning of fluxes. Biogeochemistry 51:33–69.

Grosse G, Harden J, Turetsky M, McGuire AD, Camill P, Tarnocai C, Frolking S, Schuur EAG, Jorgenson T, Marchenk S, Romanovsky V, Wickland K, French N, Waldrop M, Bourgeau-Chavez, Striegl RG. 2011. Vulnerability of high-latitude soil organic carbon in North America to disturbance. J Geophys Res-Biogeosci 116:G00K06. doi: 10.1029/2010JG001507.

Halsey LA, Vitt DH, Zoltai SC. 1995. Disequilibrium response of permafrost in boreal continental western Canada to climate change. Clim Change 30:57–73.

Harden JW, Sundquist ET, Stallard RF, Mark RK. 1992. Dynamics of soil carbon deglaciation of the Laurentide Ice Sheet. Science 258:1921–4.

Harden JW, O'Neill KP, Trumbore SE, Veldhuis H, Stocks BJ. 1997. Moss and soil contributions to annual net carbon flux of a maturing boreal forest. J Geophys Res 102:28805–16.

Harden JW, Trumbore SE, Stocks BJ, Hirsch A, Gower ST, O'Neill KP, Kasischke ES. 2000. The role of fire in the boreal carbon budget. Glob Change Biol 6(Suppl. 1):174–184.

Hayes DJ, McGuire AD, Kicklighter DW, Gurney KR, Burnside TJ, Melillo JM. 2011. Is the northern high latitude land-based CO_2 sink weakening? Global Biogeochem Cycles 25:GB3018. doi: 2010GB003813.

Hugelius G, Kuhry P. 2009. Landscape partitioning and environmental gradient analysis of soil organic carbon in a permafrost environment. Glob Biogeochem Cycles 23:GB3006. doi:10.1029/2008GB003419.

Ise T, Dunn AL, Wofsy SC, Moorcroft PR. 2008. High sensitivity of peat decomposition to climate change through water-table feedback. Nat Geosci 1:763–6.

Jorgenson MT, Osterkamp TE. 2005. Response of boreal ecosystems to varying modes of permafrost degradation. Can J For Res 35:2100–11.

Jorgenson MT, Racine CH, Walters JC, Osterkamp TE. 2001. Permafrost degradation and ecological changes associated with a warming climate in Central Alaska. Clim Change 48:551–79.

Jorgenson MT, Shur YL, Osterkamp TE, George T. 2007. Nature and extent of permafrost degradation in the discontinuous permafrost zone of Alaska. In: Proceedings of seventh international conference on global change: connection to the Arctic (GCCA-7). International Arctic Research Center, University of Alaska Fairbanks.

Jorgenson MT, Romanovsky V, Harden J, Shur Y, O'Donnell J, Schuur EAG, Kanevskiy M, Marchenko S. 2010. Resilience and vulnerability of permafrost to climate change. Can J For Res 40:1219–36.

Kane ES, Valentine DW, Michaelson GJ, Fox JD, Ping C-L. 2006. Controls over pathways of carbon efflux from soils along climate and black spruce productivity gradients in interior Alaska. Soil Biol Biochem 38:1438–50.

Kanevskiy M, Shur Y, Fortier D, Jorgenson MT, Stephani E. 2011. Cryostratigraphy of late Pleistocene syngenetic permafrost (yedoma) in northern Alaska, Itkillik River exposure. Quat Res. doi:10.1016/j.yqres.2010.12.003.

Lachenbruch AH, Brewer MC, Greene GW, Marshall BV. 1962. Temperatures in permafrost. In: Herzfeld CM, Ed. Temperature: its measurement and control in science and industry, Vol 3, part 1. New York: Reinhold. p 791–803.

Lawrence DM, Slater AG, Romanovsky VE, Nicolsky DJ. 2008. Sensitivity of a model projection of near-surface permafrost degradation to soil column depth and representation of soil organic matter. J Geophys Res 113:F02011. doi:10.1029/2007JF000883.

Limpens J, Berendse F, Blodau C, Canadell JG, Freeman C, Holden J, Roulet N, Rydin H, Schaepman-Strub G. 2008. Peatlands and the carbon cycle: from local processes to global implications—a synthesis. Biogeosciences 5:1475–91.

Ling F, Zhang T. 2003. Numerical simulation of permafrost thermal regime and talik development under shallow lakes on the Alaskan Arctic Coastal Plain. J Geophys Res 108. doi:10.1029/2002JD003014.

Ling F, Zhang T. 2004. Modeling study of talik freeze-up and permafrost response under drained thaw lakes on the Alaskan Arctic Coastal Plain. J Geophys Res 109. doi:10/1029/2003JD003886.

McGuire AD, Anderson LG, Christensen TR, Dallimore S, Guo L, Hayes DJ, Heimann M, Lorenson TD, Macdonald RW, Roulet N. 2009. Sensitivity of the carbon cycle in the Arctic to climate change. Ecol Monogr 79:523–55.

McGuire AD, Hayes DJ, Kicklighter DW, Manizza M, Zhuang Q, Chen M, Follows MJ, Gurney KR, McClelland JW, Melillo JM, Peterson BJ, Prinn R. 2010. An analysis of the carbon balance of the Arctic Basin from 1997 to 2006. Tellus 62B:455–74.

Myers-Smith IH, Harden JW, Wilmking M, Fuller CC, McGuire AD, Chapin FSIII. 2008. Wetland succession in a permafrost collapse: interactions between fire and thermokarst. Biogeosciences 5:1273–86.

Nilsson M, Klarqvist M, Bohlin E, Possnert G. 2001. Variation in 14C age of macrofossils and different fractions of minute peat samples dated by AMS. Holocene 11:579–86.

O'Donnell JA, Harden JW, McGuire AD, Kanevskiy MZ, Jorgenson MT, Xu X. 2011. The effect of fire and permafrost interactions on soil carbon accumulation in an upland black spruce ecosystem of interior Alaska: implications for post-thaw carbon loss. Glob Change Biol 17:1461–74.

O'Neill KP, Kasischke ES, Richter DD. 2003. Seasonal and decadal patterns of soil carbon uptake and emission along an age sequence of burned black spruce stands in interior Alaska. J Geophys Res 108. doi:10.1029/2001JD000443.

Olsson I. 1986. Radiometric methods. In: Berglund B, Ed. Handbook of Holocene paleoecology and paleohydrology. New York: Wiley. p 273–312.

Payette S, Delwaide A, Caccianiga M, Beauchemin M. 2004. Accelerated thawing of subarctic peatland permafrost over the last 50 years. Geophys Res Lett 31. doi:10.1029/2004GL020358.

Rivkina E, Friedmann E, McKay C, Gilichinsky D. 2000. Metabolic activity of permafrost bacteria below the freezing point. Appl Environ Microbiol 66:3230–3.

Robinson SD, Moore TR. 1999. Carbon and peat accumulation over the past 1200 years in a landscape with discontinuous permafrost, northwest Canada. Global Biogeochem Cycles 13:591–601.

Robinson SD, Moore TR. 2000. The influence of permafrost and fire upon carbon accumulation in high boreal peatlands, Northwest Territories, Canada. Arct Antarct Alp Res 32:155–66.

Romanovsky VE, Osterkamp TE. 2000. Effects of unfrozen water on heat and mass transport processes in the active layer and permafrost. Permafrost Periglac Process 11:219–39.

Schuur EAG, Bockheim J, Canadell JG, Euskirchen E, Field CB, Goryachkin SV, Hagemann S, Kuhry P, Lafleur PM, Lee H, Mazhitova G, Nelson FE, Rinke A, Romanovsky VE, Shiklomanov N, Tarnocai C, Venevsky S, Vogel JG, Zimov SA. 2008. Vulnerability of permafrost carbon to climate change: implications for the global carbon cycle. Bioscience 58:701–14.

Shur YL, Jorgenson MT. 1998. Cryostructure development on the floodplain of the Colville River Delta, Northern Alaska. In: PERMAFROST-seventh international conference (proceedings). Yellowknife, Canada. Collection Nordicana 1998. pp 993–9.

Smith LC, MacDonald GM, Velichko AA, Beilman DW, Borisova OK, Frey KE, Kremenetski KV, Sheng Y. 2004. Siberian peatlands a net carbon sink and global methane source since the early Holocene. Science 303. doi:10.1126/science.1090553.

Soil Classification Working Group. 1998. The Canadian system of soil classification. Ottawa (ON): NRC Canada Research Press. 187 pp.

Soil Survey Staff. 1998. Keys to soil taxonomy. Blacksburg (VA): Pocahontas Press, Inc. 599 pp.

Southon J, Santos G, Druffel-Rodriguez K, Druffel E, Trumbore S, Xu X, Griffin S, Ali S, Mazon M. 2004. The Keck Carbon Cycle AMS laboratory, University of California Irvine: initial operation and background surprise. Radiocarbon 46:41–9.

Stuiver M, Polach HA. 1977. Discussion: reporting of ^{14}C data. Radiocarbon 19:355–63.

Tarnocai C. 2006. The effect of climate change on carbon in Canadian peatlands. Global Planet Change 53:222–32.

Tarnocai, C., Ping C-L, Kimble J. 2007. Carbon Cycles in the Permafrost region of North America. King AW, Dilling L, Zimmerman GP, Fairman DM, Houghton RA, Marland G, Rose AZ, Wilbanks TJ, Eds. The First State of the Carbon Cycle Report (SOCCR): The North American Carbon Budget and Implications for the Global Carbon Cycle. A Report by the U.S. Climate Change Science Program and the Subcommittee on Global Change Research. Asheville (NC): National Oceanic and Atmospheric Administration, National Climatic Data Center. pp. 127–38.

Tarnocai C, Canadell JG, Schuur EAG, Kuhry P, Mazhitova G, Zimov S. 2009. Soil organic carbon pools in the northern circumpolar permafrost region. Glob Biogeochem Cycles 23. doi:1029/2008GB003327.

Thie J. 1974. Distribution of thawing permafrost in the southern part of the discontinuous permafrost zone in Manitoba. Arctic 27:189–200.

Trumbore SE. 2000. Age of soil organic matter and soil respiration: radiocarbon constraints on belowground C dynamics. Ecol Appl 10:399–411.

Trumbore SE, Harden JW. 1997. Accumulation and turnover of carbon in organic and mineral soils of the BOREAS northern study area. J Geophys Res 102:28817–30.

Turetsky M, Wieder K, Halsey L, Vitt D. 2002a. Current disturbance and the diminishing peatland carbon sink. Geophys Res Lett 29. doi:10.1029/2001GL014000.

Turetsky MR, Wieder RK, Vitt DH. 2002b. Boreal peatland C fluxes under varying permafrost regimes. Soil Biol Biochem 34:907–12.

Turetsky MR, Wieder RK, Vitt DH, Evans RJ, Scott KD. 2007. The disappearance of relict permafrost in boreal North America: effects of peatland carbon storage and fluxes. Glob Change Biol 13:1922–34.

Van Cleve K, Dyrness CT, Viereck LA, Fox J, Chapin FSIII, Oechel W. 1983. Taiga ecosystems in interior Alaska. Bioscience 33:39–44.

Waddington JM, Roulet NT. 1997. Groundwater flow and dissolved carbon movement in a boreal peatland. J Hydrol 191:122–38.

Waldrop MP, Wickland KP, White RIII, Berhe AA, Harden JW, Romanovsky VE. 2010. Molecular investigations into a globally important carbon pool: permafrost-protected carbon in Alaskan soils. Glob Change Biol 16:2543–54.

Wang C, Bond-Lamberty B, Gower ST. 2003. Carbon distribution of a well- and poorly-drained black spruce chronosequence. Glob Change Biol 9:1066–79.

West JJ, Plug LJ. 2008. Time-dependent morphology of thaw lakes and taliks in deep and shallow ground ice. J Geophys Res 113. doi:10.1029/2006JF000696.

Wickland KP, Striegl RG, Neff JC, Sachs T. 2006. Effects of permafrost melting on CO2 and CH4 exchange of a poorly drained black spruce lowland. J Geophys Res 111. doi:10.1029/2005JG000099.

Xu X, Trumbore SE, Zheng S, Southon JR, McDuffee KE, Luttgen M, Liu JC. 2007. Modifying a sealed tube zinc reduction method for preparation of AMS graphite targets: reducing background and attaining high precision. Nucl Instrum Methods Phys Res B 259:320–9.

Yoshikawa K, Hinzman LD. 2003. Shrinking thermokarst ponds and groundwater dynamics in discontinuous permafrost near Council, Alaska. Permafrost Periglac Process 14:151–60.

Zhuang Q, McGuire AD, O'Neill KP, Harden JW, Romanovsky VE, Yarie J. 2002. J Geophys Res Atmos 108, 8147. doi:10.1029/2001JD001244.

Zoltai SC. 1993. Cyclic development of permafrost in the peatlands of Northwestern Alberta, Canada. Arctic Alpine Res 25:240–6.

Zoltai SC, Vitt DH. 1990. Holocene climatic change and the distribution of peatlands in western interior Canada. Quat Res 33:231–40.